Spin-orbit coupling and tunneling current in a parabolic quantum dot

Hong-Yi Chen,[1] Vadim Apalkov,[2] and Tapash Chakraborty[1]
[1]*Department of Physics and Astronomy, University of Manitoba, Winnipeg, Canada MB R3T 2N2*
[2]*Department of Physics and Astronomy, Georgia State University, Atlanta, Georgia 30303, USA*
(Received 24 October 2006; revised manuscript received 26 December 2006; published 4 May 2007)

We propose an approach to explore the signature of the spin-orbit interaction in a quantum dot subjected to a tilted magnetic field. The spin-orbit coupling within the dot manifests itself as an anticrossing of the energy levels as the tilt angle is varied. The anticrossing gap has a nonmonotonic dependence on the magnitude of the magnetic field and exhibits a peak at some finite values of the magnetic field. From the dependence of the tunneling current through the quantum dot on the bias voltage and the tilt angle, the anticrossing gap, and most importantly the spin-orbit coupling strength, can be determined.

DOI: 10.1103/PhysRevB.75.193303 PACS number(s): 73.40.Gk, 72.25.Dc, 71.70.Ej

In recent years, there has been a well-concerted effort to achieve a coherent control on the electron spin transport in semiconductor nanostructures because of its attractive potential for future spin-based electronic devices.[1] The spin-orbit (SO) interaction plays a crucial role in that pursuit, as it provides a means for coupling of the electron spin to its orbital motion. The SO interaction may in turn be manipulated by applying a gate voltage. Studies of the SO coupling effects in parabolic quantum dots (QDs) are equally intriguing[2,3] because one expects that such a system will provide the important step toward quantum information processing.[4] In narrow-gap semiconductors such as the InAs-based system, the dominant source of the SO interaction is the structural inversion asymmetry.[5] The resultant Bychkov-Rashba type of SO interaction[6] is the interaction of our choice here. The most common method of determining the strength of the SO coupling is to study the beating pattern in Shubnikov–de Haas (SdH) oscillations.[7] However, that process does not always provide an unambiguous determination of the SO coupling strength.

In this paper, we propose an approach to determine the strength of the SO interaction in the QDs. It is based on an analysis of the behavior of the electronic QD energy levels in a tilted magnetic field. The tilted magnetic field has an advantage over parallel and perpendicular fields because it introduces the Zeeman splitting of the energy levels and modifies the orbital motion of the electron within the QD as well. The relative strength of these two contributions in the electron dynamics can be varied by changing the tilt angle. Without the SO interaction, the energy spectrum of the QD has a strong dependence on the direction of the magnetic field, thus exhibiting regions of level crossings at different tilt angles. The levels that cross have the opposite spin directions, and without the SO interaction there is no mixing between them. The SO interaction couples the different spin states. In this case we should expect an anticrossing of the energy levels as a function of the tilt angle. Interestingly, the strength of the anticrossing characterizes the strength of the SO coupling. The most accurate way to study experimentally the structure of the energy spectra around the anticrossing region is to measure the tunneling current through the quantum dot. Transport spectroscopy is a powerful tool to study a variety of phenomena related to the correlation and interaction effects in a QD.[8] The main idea of the tunneling spectroscopy at a finite bias voltage is that the tunneling current depends on the number of available (for tunneling) channels in the QD. In the following, we study the tunneling transport through a QD in a tilted magnetic field and show that the tunneling current is dependent on the tilt angle and the bias voltage within the anticrossing region.

The energy range of the anticrossing region is usually smaller than the energy of the interelectron interaction, which can be estimated to be about 7 meV.[3] The tunneling process can then be described by a single-electron picture. The Hamiltonian of an electron in a parabolic QD in a tilted magnetic field is

$$H = \frac{1}{2m^*}\left(\mathbf{p} + \frac{e}{c}\mathbf{A}\right)^2 + \frac{1}{2}m^*\omega_0^2 r^2 + \frac{1}{2}g\mu_B B_z\sigma_z + \frac{\alpha}{\hbar}\left[\sigma \times \left(\mathbf{p} + \frac{e}{c}\mathbf{A}\right)\right]_z + \frac{1}{2}g\mu_B B_x\sigma_x,$$

where $\mathbf{A} = \frac{1}{2}B_z(-y,x,0)$ is the vector potential in the symmetric gauge, $-e$ is the electron charge, α is the SO coupling strength, g is the effective Landé g factor, and $\mathbf{p}$ is the two-dimensional vector in the (x,y) plane. We have assumed that there is no dynamics in the z direction due to the size quantization and the electron occupies the corresponding lowest subband. The value of α obtained from various experiments lie in the range of 5–45 meV nm.[7] In a tilted field, the perpendicular component is $B_z = B\cos\theta$ while the parallel component is $B_x = B\sin\theta$, where B is the magnitude of the magnetic field and θ is the angle between the magnetic field vector and the z axis. In the above expression for the vector potential $\mathbf{A}$, we have taken into account only the perpendicular component of the magnetic field B_z. Since the size of the dot in the z direction is small, the only effect of the parallel field is through the Zeeman energy. The energy spectra and the wave functions corresponding to the above Hamiltonian (but for a zero tilt angle) have been obtained earlier numerically.[3] All the calculations below have been performed for the case of the InAs quantum dots. It should be pointed out that titled-field experiments on the QDs have been reported earlier in the literature,[9] but without any consideration of the SO coupling.

In our approach, a QD is attached through the tunneling

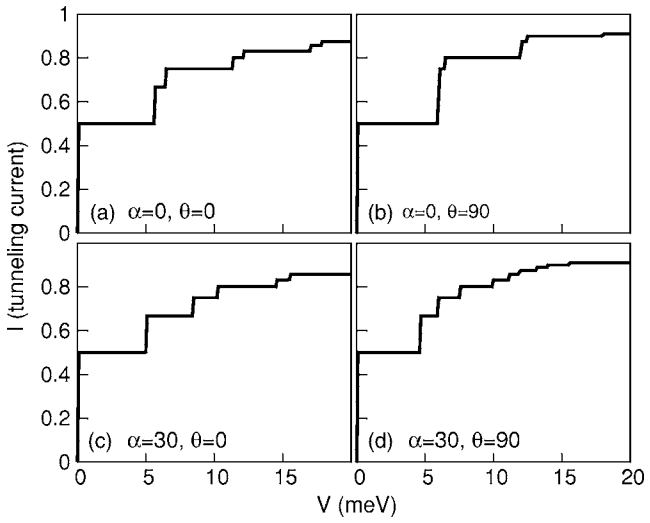

FIG. 1. Tunneling current vs the bias voltage for four different cases at $B=4$ T: (a) $\alpha=0$, $\theta=0$; (b) $\alpha=0$, $\theta=90°$; (c) $\alpha=30$ meV nm, $\theta=0$; (d) $\alpha=30$ meV nm, $\theta=90°$. The parameters for the InAs QDs are $m^*/m_0=0.042$, $g=-14$, and the confinement potential strength is $\hbar\omega_0=3.0$ meV.

barriers to the right and left leads. We study the tunneling current through the dot at a finite bias voltage between the leads. The tunneling process through a parabolic QD is described as a sequential single-electron tunneling.[10] The QD is charactrized by the probability P_0 that there are no electrons in the dot and probabilities $P_i, i=1,\ldots,N$ that the electron occupies an energy level E_i in the dot. For the probabilitiy P_i we can write the rate equations in the form

$$\frac{\partial P_0}{\partial t} = -P_0\sum_{i=1}^{N} W_i + \sum_{i=1}^{N} P_i V_i, \tag{1}$$

$$\frac{\partial P_i}{\partial t} = -P_i V_i + W_i P_0, \tag{2}$$

$$P_0 + P_1 + P_2 + \cdots + P_N = 1, \tag{3}$$

where the last equation is the normalization condition. The transition rates W_i and V_i are the rates of tunneling in and out of the dot, respectively. These rates can be found from the Fermi golden rule

$$W_i = \Gamma f_L(E_i) + \Gamma f_R(E_i),$$

$$V_i = \Gamma[1 - f_L(E_i)) + \Gamma(1 - f_R(E_i)\ ],$$

where Γ is the tunneling rate, which we assume to be energy independent and is also the same for both left and right leads. The rate equations (1)–(3) are valid for $\Gamma \ll kT$, where T is the temperature and k is the Boltzmann constant. Here $f_L(E)$ and $f_R(E)$ are the Fermi distribution functions of the left (L) and right (R) leads, respectively. The chemical potentials of the left and right leads are μ_L and μ_R, respectively. In what follows, we have chosen the ground state of a QD with a single electron as the zero-energy state. The temperature in our calculation is ~0.1 K.

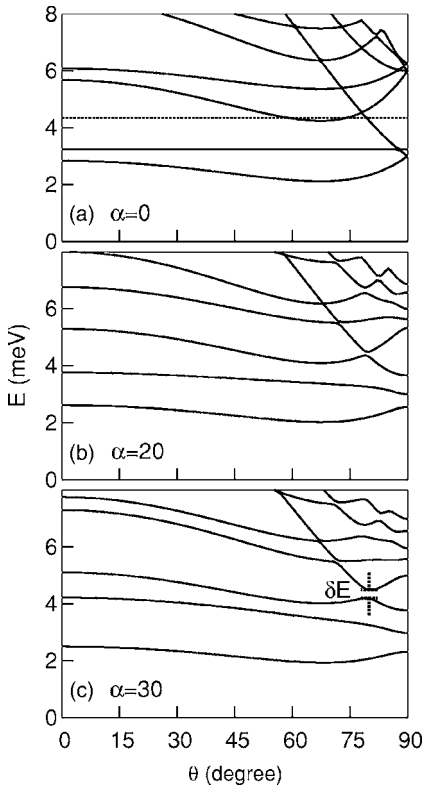

FIG. 2. The energy spectra as a function of the tilt angle (θ) for $B=4$ T and for different values of the SO coupling strength: (a) $\alpha=0$, (b) $\alpha=20$, and (c) $\alpha=30$ meV nm. The dashed line in (a) corresponds to the energy $E=4.3$ meV. In (c), δE is the energy gap.

For the stationary case, the time derivatives of P_0 and P_i are zero. Then the linear system of equations Eqs. (1)–(3) can be easily solved and the stationary tunneling current can be found from $I(V)=\Sigma_{i=1}^{N}(W_i^L P_0 - V_i^L P_i)$, where V is the bias voltage and the chemical potentials μ_L and μ_R are related to V as $\mu_L=V/2$ and $\mu_R=-V/2$.

In Fig. 1, we show the tunneling current as a function of the bias voltage for four different cases. These cases are divided into two groups by the angle of the applied tilted magnetic field: (i) ($\theta=0°$) and (ii) ($\theta=90°$). In the first case, Fig. 1(a) and Fig. 1(c) do not show any significant difference when the SO interaction is included, while in the second case the presence of the SO interaction lifts the degenerate states which creates more steps in the I-V curve [as seen in Fig. 1(b) and Fig. 1(d)].

From Fig. 1 it is clear that by varying the tilt angle θ one can make a significant change in the I-V curve. In order to study the effect of a tilted field, we have looked at the angle dependence of the energy levels. Figure 2(a) shows several level crossings in the absence of the SO coupling. The first crossing appears around $E=4.5$ meV and θ between 70° and 90°. In the presence of the SO coupling [Fig. 2(b)], that level crossing becomes an anticrossing with an energy gap of δE. Figure 2(c) shows that the energy gap increases with an increase of α. The anticrossing in Fig. 2 is a direct manifestation of the SO interaction. We now demonstrate that the anticrossing of the energy levels results in a specific dependence of the tunneling current on the bias voltage and the tilt angle.

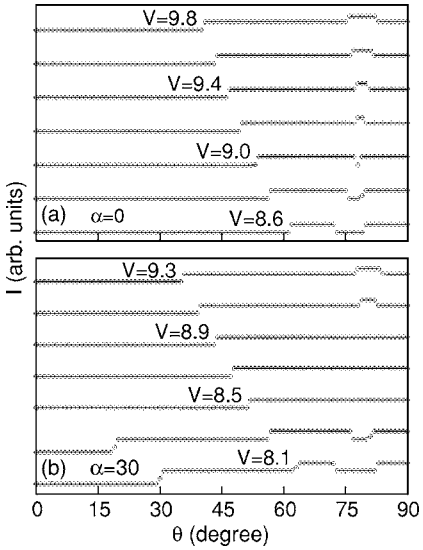

FIG. 3. Tunneling current as a function of the tilt angle θ at $B=4$ T and for (a) $\alpha=0$, and (b) $\alpha=30$ meV nm. Each line corresponds to a constant bias voltage V. The bias voltage is expressed in meV. The increment of the voltage is 0.2 meV. The curves have been shifted vertically for clarity.

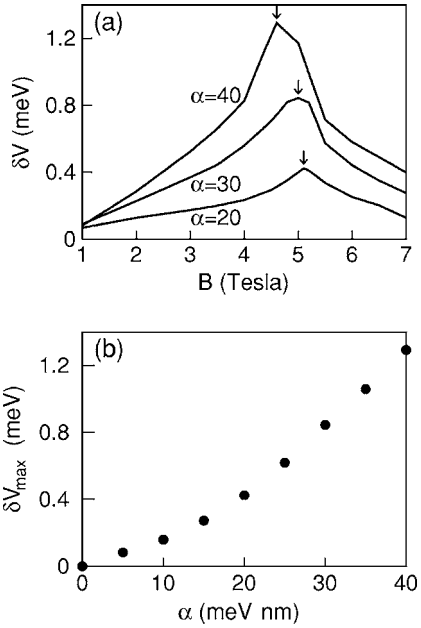

FIG. 4. (a) The magnetic field dependence of the voltage difference δV for three different values of the SO coupling strength: $\alpha=20$, 30, and 40 meV nm. The corresponding peak positions are at $B=5.1$, 5.0, and 4.6 T for $\alpha=20$, 30, and 40, respectively. (b) The SO coupling strength dependence on the maximum voltage difference, $\delta V_{\max}$. Each point corresponds to a different value of the magnetic field.

The tunneling current as a function of θ is shown in Fig. 3. In Fig. 3(a) we present the data for the tunneling current at different bias voltages with an increment of 0.2 meV for the QD without a SO coupling. At $V=8.6$ meV ($\mu_L=4.3$ meV), the Fermi energy of the left lead μ_L is below the first level crossing, which is illustrated by the dashed line in Fig. 2(a). Around $\theta=70°$, there are three levels of the QD below μ_L. As we increase θ, the Fermi energy of the left lead goes below the third energy level. At this point, the tunneling current which depends on the number of levels between the Fermi energies of the left and right leads, drops. However, when $\theta \geqslant 80°$, the Fermi energy μ_L is again above the third energy level. The tunneling current then goes up. The tunneling current as a function of the tilt angle then shows a dip at the voltage below the crossing point. When we increase the voltage and approach the crossing point, the dip becomes narrower. Just above the crossing point, the tunneling current shows a narrow bump similar to that at $V=9.2$ meV in Fig. 3(a). With a further increase of the bias voltage the bump in the tunneling current becomes wider.

Figure 3(b) shows the tunneling current for a finite value of the SO coupling strength $\alpha=30$ meV nm. Just as for the system without the SO interaction, the tunneling current reveals a dip when the bias voltage is less than 8.3 meV. With an increase of the voltage, the system shows a behavior characteristic of that of the level anticrossing. Namely, within a finite interval of the bias voltages $\delta V=2\delta E$, the tunneling current becomes independent of the tilt angle. This corresponds to the case where the Fermi energy of the left lead is in the anticrossing gap. If the voltage is continuously increased, the flat pattern disappears and in its place a bump pattern emerges. This change of the pattern is evidence for the existence of the SO coupling which opens a gap at the crossing point [see Fig. 2(c)]. The dip occurs when the voltage is below the bottom edge of the energy gap, while the flat curve appears when the voltage is inside the gap. The bump in the curve means that the voltage is above the top edge of the energy gap. The change of pattern from a dip to being flat and then to a bump can be quantified by the voltage difference δV. Since $\delta V=2\delta E$, this voltage difference will determine the strength of the SO coupling α.

Analyzing the tunneling current versus the angles, we are able to directly evaluate α. However, the anticrossing energy gap also depends on the magnitude of the applied magnetic field. With an increasing magnetic field, the size of the energy gap increases and reaches a maximum value $\delta E_{\max} = \delta V_{\max}/2$. Figure 4(a) illustrates the above trend for three different values of α. For larger values of α the peak is located at a lower magnetic field. The peak shifts toward a higher field as the SO coupling strength decreases. The peak values are all located between $B=4.5$ T and $B=5.5$ T. The optimal value of the magnetic field illustrates the interplay between the orbital and spin effects of the magnetic field. In Fig. 4(b) the value of $\delta V_{\max}$ at the optimal magnetic field is shown as a function of α. Note that at different values of α the optimal magnetic field is different in Fig. 4(b). With the known maximum value of the voltage differences, $\delta V_{\max}$, the corresponding α can be directly determined.

For a perpendicular magnetic field the energy spectra also shows the anticrossing behavior. Just as for the tilted field, this should also result in the corresponding structure in the tunneling I-V dependence. Application of a tilted magnetic field has some advantage however: in a perpendicular field the anticrossing structure is observed only at one value of the magnetic field and we need to change the magnitude of the magnetic field to see the anticrossing behavior. In a tilted

field the anticrossing behavior exists at all values of the magnetic field greater than a certain critical value. Another advantage of the tilted field is that the magnitude of δV, or the magnitude of the anticrossing gap, is larger in the tilted magnetic field, which would make it easier to observe this effect. As an example, for $\alpha=20$ meV nm, the anticrossing gap in the perpendicular field is ~ 0.23 meV, while the maximum anticrossing gap in the tilted field is 0.41 meV. This also means that the maximum value of the anticrossing gap [Fig. 4(a)] should be observed at a nonzero tilt angle. Indeed for $\alpha=20$ meV nm the maximum δV is realized at $\theta=83$. The reason why the anticrossing gap is larger in a tilted magnetic field and why there is a maximum in the dependence of the anticrossing gap on the tilt angle is because the tilted magnetic field introduces a mixture of the spin and orbital effects of the magnetic field. The parallel component of the tilted magnetic field results only in the Zeeman splitting, while the perpendicular component modifies the orbital motion within the dot plane. The SO coupling introduces a mixture between the states with different directions of spin. The smaller the energy separation between the states, the stronger is the SO mixture between the states. Due to the Zeeman energy, the parallel magnetic field suppresses the energy difference between the states with different spin and effectively increases the SO coupling between the states.

There are a few effects that we did not take into account here. The first is the effect of the parallel component of the tilted magnetic field on the tunneling rates. This is justified as long as the magnetic length is much larger than the size of the system in the z direction, i.e., much larger than the quantum dot height and the width of the tunneling barriers. For a 4 T magnetic field this assumption is consistent with experimentally studied self-assembled InAs quantum dots, for which the diameter is 20–30 nm and a typical height of 4–10 nm.[11] We also assume that the confinement potential of the dot is parabolic and ignored the nonparabolicity of the energy spectra in the Hamiltonian. We have also ignored the dependence of the g-factor on the tilt angle, and the effects of the strain on the energy spectra of the dot. For realistic QDs, all these factors should be taken into account to evaluate the anticrossing gap. The size parameters of quantum dots used in our calculations are consistent with the dot sizes, i.e., diameter 20–30 nm, of self-assembled InAs quantum dots.[11] Our primary goal here is to illustrate the main message of our present work: in order to study the signature of SO coupling in the tunneling experiments in a magnetic field, one needs to apply a *tilted magnetic field* to have the largest anticrossing gaps in the energy spectra. The actual value of this gap may, however, depend on the type of materials and on the precise structure of the dots.

H.Y.C. would like to thank P. Pietiläinen for helpful discussions. This work has been supported by the Canada Research Chair Program, a Canadian Foundation for Innovation grant, and the NSERC Discovery grant.

[1] D. Grundler, Phys. World **15**(4), 39 (2002); S. A. Wolf *et al.*, Science **294**, 1488 (2001); G. Schmidt, C. Gould, and L. W. Molenkamp, Physica E (Amsterdam) **25**, 150 (2004).

[2] T. Chakraborty and P. Pietiläinen, Phys. Rev. Lett. **95**, 136603 (2005); Phys. Rev. B **71**, 113305 (2005).

[3] P. Pietiläinen and T. Chakraborty, Phys. Rev. B **73**, 155315 (2006), and references therein.

[4] D. Loss, G. Burkard, and D. P. DiVincenzo, J. Nanopart. Res. **2**, 401 (2000).

[5] W. Zawadzki and P. Pfeffer, Semicond. Sci. Technol. **19**, R1 (2004).

[6] Yu. A. Bychkov and E. I. Rashba, Pis'ma Zh. Eksp. Teor. Fiz. **39**, 64 (1984) [JETP Lett. **39**, 78 (1984)].

[7] D. Grundler, Phys. Rev. Lett. **84**, 6074 (2000); J. Nitta *et al.*, *ibid.* **78**, 1335 (1997); T. Matsuyama *et al.*, Phys. Rev. B **65**, 155322 (2002).

[8] J. Weis, R. J. Haug, K. v. Klitzing, and K. Ploog, Phys. Rev. Lett. **71**, 4019 (1993); T. Schmidt *et al.*, Phys. Rev. B **51**, 5570 (1995); M. Narihiro *et al.*, Appl. Phys. Lett. **70**, 105 (1997); N. Horiguchi *et al.*, *ibid.* **70**, 2294 (1997); A. S. G. Thornton *et al.*, *ibid.* **73**, 354 (1998); S. Tarucha *et al.*, Phys. Rev. Lett. **84**, 2485 (2000); T. Ota *et al.*, *ibid.* **93**, 066801 (2004); **95**, 236801 (2005); J. Konemann *et al.*, *ibid.* **94**, 226404 (2005); K. H. Schmidt *et al.*, Phys. Rev. B **62**, 15879 (2000).

[9] J.-M. Meyer *et al.*, Phys. Status Solidi B **224**, 685 (2001); B. Meurer, D. Heitmann, and K. Ploog, Surf. Sci. **305**, 610 (1994).

[10] S. Luryi, Appl. Phys. Lett. **47**, 490 (1985).

[11] B. Krause *et al.*, Phys. Rev. B **72**, 085339 (2005); A. V. Baranov *et al.*, *ibid.* **68**, 205318 (2003).